Tracing groundwater recharge sources in the northwestern Indian alluvial aquifer using water isotopes ($\delta^{18}O$, $\delta^{2}H$ and ^{3}H)

Suneel Kumar Joshi[1], Shive Prakash Rai[2, *], Rajiv Sinha[1,*], Sanjeev Gupta[3], Alexander Logan Densmore[4], Yadhvir Singh Rawat[2], Shashank Shekhar[5]

[1]Department of Earth Sciences, Indian Institute of Technology, Kanpur, 208016, India, [2]National Institute of Hydrology, Roorkee, India, [3]Department of Earth Science and Engineering, Imperial College London, London, SW7 2AZ, United Kingdom, [4]Institute of Hazard, Risk, and Resilience and Department of Geography, Durham University, Durham, DH1 3LE, United Kingdom, [5]Department of Geology, University of Delhi, Delhi, 110007, India

Abstract

Rapid groundwater depletion from the northwestern Indian aquifer system in the western Indo-Gangetic basin has raised serious concerns over the sustainability of groundwater and the livelihoods that depend on it. Sustainable management of this aquifer system requires that we understand the sources and rates of groundwater recharge, however, both these parameters are poorly constrained in this region. Here we analyse the isotopic ($\delta^{18}O$, $\delta^{2}H$ and tritium) compositions of groundwater, precipitation, river and canal water to identify the recharge sources, zones of recharge, and groundwater flow in the Ghaggar River basin, which lies between the Himalayan-fed Yamuna and Sutlej River systems in northwestern India. Our results reveal that local

[*] Corresponding author email: sprai1966roorkee@gmail.com; rsinha@iitk.ac.in

precipitation is the main source of groundwater recharge. However, depleted $\delta^{18}O$ and $\delta^{2}H$ signatures at some sites indicate recharge from canal seepage and irrigation return flow. The spatial variability of $\delta^{18}O$, $\delta^{2}H$, d-excess, and tritium reflects limited lateral connectivity due to the heterogeneous and anisotropic nature of the aquifer system in the study area. The variation of tritium concentration with depth suggests that groundwater above c. 80 mbgl is generally modern water. In contrast, water from below c. 80 mbgl is a mixture of modern and old waters, and indicates longer residence time in comparison to groundwater above c. 80 mbgl. Isotopic signatures of $\delta^{18}O$, $\delta^{2}H$ and tritium suggest significant vertical recharge down to a depth of 320 mbgl. The spatial and vertical variations of isotopic signature of groundwater reveal two distinct flow patterns in the aquifer system: (i) local flow (above c.80 mbgl) throughout the study area, and (ii) intermediate and regional flow (below c. 80 mbgl), where water recharges aquifers through large-scale lateral flow as well as vertical infiltration. The understanding of spatial and vertical recharge processes of groundwater in the study area provides important base-line knowledge for developing a sustainable groundwater management plan for the northwestern Indian aquifer system.

Keywords: Water isotopes, recharge sources, recharge zones, groundwater flow, northwestern Indian aquifer.

1. Introduction

Groundwater depletion from major alluvial aquifer systems is a global issue (e.g., Foster and Chilton, 2003; Wada et al., 2012; Gleeson et al., 2015). The global groundwater extraction rate is ~1500 km^3 per year (Doll et al., 2012), which is more than the natural groundwater recharge rate. Increasing water demand for economic development, power generation, drinking water, and agriculture has exacerbated groundwater exploitation, leading to the decline of the water table in major alluvial aquifer systems across the world (Konikow and Kendy, 2005; Aeschbach-Hertig and Gleeson, 2012). Large-scale groundwater depletion has resulted in land subsidence, reduction in the base flow of springs and rivers during dry periods, saltwater intrusion, water quality degradation, and damage to aquatic ecosystems in different parts of the world (Fishman et al., 2011). This problem is becoming more challenging given the increasing demands by development and a growing population, along with poorly understood effects of climate-driven changes in the water cycle (e.g., Aeschbach-Hertig and Gleeson, 2012). These broad issues can be addressed only if we know the sources and areas of groundwater recharge along with the interconnectivity and dynamics of aquifer systems at appropriate regional scales. This information, however, is poorly constrained for many of the world's major alluvial aquifer systems.

The northwestern Indian aquifer system (NWIA) underlies the states of Punjab, Haryana, and Rajasthan and represents one of the major alluvial aquifer systems of the Indo-Gangetic basin in northern India and Pakistan (MacDonald et al., 2016). The region is characterised by multiple, semi-confined sand-rich aquifer bodies that are laterally discontinuous but may be highly interconnected (van Dijk et al., 2016a; MacDonald et al., 2016). This is one of the most agriculturally intensive regions in India, where annual food grain production has increased four-fold from 50 million tons in 1950 to 203 million tons in 1999-2000 (Kumar et al., 2005). Such intensive agricultural activities are mainly attributed to the so-called 'green revolution' in India, aimed at achieving self-reliance in food production. This intensive food production has led, however, to greatly-accelerated demand for irrigation water. Since India's surface water infrastructure was never adequate to meet this requirement, the focus shifted to groundwater extraction using large numbers of tube wells. The average tube well density in this region is >15 km^{-2} (Ambast et al., 2006). As a consequence, the groundwater level in the NWIA is declining at a much higher rate than any other comparably-sized aquifer on the Earth (Rodell et al., 2009; Tiwari et al., 2009; Chen et al., 2014; Panda and Wahr, 2015; Long et al., 2016). Satellite-borne gravity measurements suggest that groundwater levels declined at ~3.1±0.1 cm per year between 2005 and 2010 (Long et al., 2016) and that water was lost at a rate of ~54±9 km^3 per year between 2002 and 2008 (Tiwari et al., 2009); the average rate of groundwater depletion is ~20.4±7.1 gigatonnes per year for 10 years from 2003 to 2012 (Chen et al., 2014).

Sustainable management of the NW Indian aquifer system needs a comprehensive understanding of the sources and rates of groundwater recharge. In addition, it is also important to know the degree of spatial variability of recharge rates that is imposed by the geological heterogeneity that is inherent within alluvial settings. Water isotopes are commonly used for determining the sources of groundwater and residence times. The isotopes of hydrogen (^2H and ^3H) and oxygen (^{18}O) have proved to be particularly useful tools in hydrogeological studies, providing valuable insights into water dynamics in a given basin (Dincer et al. 1970; Fontes, 1980; Clark and Fritz, 1997; Hoque and Burgess, 2012). A few local isotopic studies in Punjab and Haryana states have focused on the provenance of groundwater using isotopic tracers, sources of groundwater salinity (Kulkarni et al., 1996; Lorenzen et al., 2012), and estimation of recharge rate based on the tritium tagging technique (Datta et al., 1996; Rangarajan and Athavale, 2000). These studies provide a broad understanding of the mechanism of local recharge sources and zones, but it is hard to extrapolate these local studies to understand basin-scale recharge mechanisms given the heterogeneity of the alluvial aquifer system (Bowen, 1985; Sinha et al. 2013; van Dijk et al., 2016a). There has been no systematic study of recharge sources, zones and groundwater flow (e.g., isotopic fingerprint or age) at an appropriate scale in this important region, with the important exception of the studies of Lapworth et al. (2015, 2017) and Rao et al. (2017) who focused on a region between the Beas and Sutlej Rivers in Punjab. Comparable work across the rest of Punjab and Haryana has not yet been done.

To investigate the spatial pattern of groundwater recharge sources in the NWIA, we focus here on the Ghaggar River basin that encompasses parts of the states of Punjab, Haryana and Rajasthan in northwestern India. We investigate the sources of groundwater recharge using the stable isotopes of oxygen and hydrogen in water, coupled with measurements of tritium radioisotopes. Our specific objectives are (1) isotopic characterization of groundwater and surface waters for the Ghaggar River basin; (2) identification of the recharge sources and zones; and (3) understanding recharge processes and groundwater flow dynamics in the aquifer system that underlies the Ghaggar River basin. To achieve our objectives, we conducted systematic sampling of precipitation, surface waters from both rivers and canals, and groundwater across the study area (Figure 1).

2. Study Area

The study area for our investigation encompasses a major area of the NWIA in the Indo-Gangetic basin, focusing on the Ghaggar River basin which lies between 29°10'N and 30º54'N and 74º20'E and 77º26'E and covers an area of 22,235 km^2 (Figure 1). The Ghaggar River originates in the Siwalik foothills of the Himalayas at an altitude of 1,927 m asl (above sea level) and flows for ~330 km across the study area. In the alluvial part of the basin, the elevation varies from 350 to 150 m asl. The Ghaggar is a seasonal river that is set within a large, slightly incised paleo-valley that is more than 3 km wide (Bhadra et al., 2009; Sinha et al., 2013; van Dijk et al., 2016a; Singh et al., 2017). About 90% of the study area is used for intensive agriculture (UNDP, 1985; Ambast et al., 2006), and the main sources of irrigation water supply are precipitation, groundwater, and surface water from canals. Water from the Sutlej River is diverted through a dense canal network for irrigation in the middle and downstream parts of the basin. Water demand in this region has greatly increased since 1970 (Kumar et al., 2014) due to a progressive shift towards rice cultivation in the monsoon season (July - September). As a result of this, a net annual water deficit of 1.63 million-hectare meters for Punjab (estimated for 2008; Kumar et al., 2014) has to be met through groundwater abstraction. As a consequence, there has been a rapid decline in the water table over much of the region over the last four decades (Rodell et al., 2009; Tiwari et al., 2009; Chen et al., 2014; Long et al., 2016; MacDonald et al., 2016).

The Ghaggar River basin extends across four geomorphic units that coincide with distinct subsurface hydrogeological units: the Siwalik hills, the Sutlej and Yamuna sediment fans, the interfan area, and spatially-restricted aeolian deposits (Figure 1). The Siwalik Hills range in altitude from 400 to 2000 m asl and are made up of sandstone and conglomerate. They are separated from sediments of the Indo-Gangetic foreland basin by the Himalayan Frontal Thrust (HFT). The foreland basin fill is dominated by fluvial fans deposited by the Sutlej and Yamuna rivers, and comprising spatially heterogeneous sand, silt, and clay deposits associated with abandoned, avulsive river channel belts (UNDP, 1985; Saini et al., 2009; Sinha et al., 2013; van Dijk et al., 2016a; Singh et al., 2017). These fans decrease in surface elevation from about 350 to 150 m asl over a distance of about 300 km. Van Dijk et al. (2016a) used aquifer-thickness logs from the Central Groundwater Board (CGWB) to show that aquifer bodies within the fans are typically composed of stacked channel deposits of fine to medium sand, interspersed both vertically and laterally with non-aquifer silt and clay. The aquifer bodies have a median thickness of about 6-7 m (van Dijk et al., 2016a). These sediments form a multi-layer aquifer system (Lapworth et al., 2017). In contrast, the interfan area between the Sutlej and Yamuna fans, east of Patiala (Figure 1), is characterised by thinner and less abundant aquifer bodies, even at locations that are adjacent to the HFT (van Dijk et al., 2016a). This geomorphic framework contrasts with the traditional division of the Indo-Gangetic basin into Siwalik Hills and distal alluvial deposits, and reflects an important along-strike stratigraphic heterogeneity in the aquifer system. The bulk specific yield varies spatially, with values of 10-26% in the interfan area near the Himalayan foothills and 5-15% in the Sutlej and Yamuna fans (UNDP, 1985; CGWB, 2009, 2012).

The climatic conditions in the Ghaggar basin range from subtropical to semi-arid, with temperatures of 25-48°C in summer, and 5-19°C in winter (Kumar et al., 2014). Precipitation shows marked spatial variation throughout the study area. Mean annual rainfall is ranges between 800-1200 mm in the Siwalik Hills, 74% of which is received during July to September. Mean annual rainfall in the foreland basin is 400-800 mm but decreases to less than 400 mm in the southwestern part of the study area.

3. Sampling strategy and measurements

We designed our sampling strategy to document spatial and vertical variation in the isotopic signature ($\delta^{18}O$, $\delta^{2}H$, and ^{3}H) of both source water (precipitation, canal water, and rivers) and groundwater across the study area (Figure 1). Water sampling was carried out throughout the study area during June and July 2013 for $\delta^{18}O$ and $\delta^{2}H$ analysis, and October-November 2012, June 2013, and April and June 2015 for ^{3}H analysis. We collected groundwater samples from 244 locations from monitoring wells of the CGWB and state groundwater departments, public tube wells, and hand pumps using a grid of about 10x10 km across the study area. The wells were purged for 30-45 minutes depending on the depth of the well before sampling. The screening depths in the sampled wells vary from ~6 to 365 mbgl. It is worth mentioning that screening depths are only recorded for government tube wells and piezometers, while depths for public tube wells and hand pumps are based on local information (tube wells and hand pumps owner). As per the hand pump / tube wells owner, there is generally some displacement (±1 to ±3 m) during the screen installation. So, we have assumed an uncertainty of ±5 m in the screen depths of such wells.

The primary recharge sources of groundwater in the study area are meteoric water, rivers, and irrigation canals. Canal water is typically abstracted from the river network at or near the Himalayan mountain front. To establish the isotopic signatures of these different sources, canal and river water samples were collected from random locations based on accessibility within the study area. Also, three rain gauge stations were set up in Chandigarh, Patiala, and Sirsa (Figure 1) to develop a local meteoric water line for the Ghaggar River basin.

All water samples were collected in pre-cleaned polypropylene bottles (20 ml for stable isotopic samples and 500 ml for tritium samples). The bottles were rinsed at the site twice with the sample water. To further avoid any diffusive and evaporative losses from the samples bottles, they were tightly sealed and brought immediately to the laboratory for isotopic analysis. Samples for $\delta^{18}O$ and $\delta^{2}H$ were analysed during August-October 2013, and those for ^{3}H were analysed during March, August, September 2013 (n=68) and during August-September 2015 (n=19). Sample latitude, longitude, and altitude were measured using a handheld Global Positioning System receiver during the sampling. Additional parameters such as pH, temperature, and electrical conductivity (EC) were also measured in the field using handheld pH and EC meters.

Stable isotopic (δ^2H, $\delta^{18}O$) and tritium (^3H) analyses were carried out at the Nuclear Hydrology Laboratory at National Institute of Hydrology (NIH) Roorkee, India. Measurements of $\delta^{18}O$ and δ^2H were made using Continuous Flow Isotope Ratio Mass Spectrometry and Dual Inlet Isotope Ratio Mass Spectrometry following standard procedures (Epstein and Mayeda, 1953; Brenninkmeijer and Morrison, 1987). The results are expressed in concentrations per mil (‰) relative to Vienna Standard Mean Ocean Water (VSMOW) on the δ scale:

$$\delta = \left(\frac{R_{sample}}{R_{standard}} - 1\right) \times 1000\ \text{‰}\ \ \text{VSMOW}$$

where R_{sample} is the $^{18}O/^{16}O$ or $^2H/^1H$ ratio of the water samples, and $R_{standard}$ is the corresponding ratio for VSMOW. The overall precision, based on ten repeated measurements of each sample, was less than ±1.0‰ for δ^2H and ±0.1‰ for $\delta^{18}O$.

We also analysed tritium (^3H) to place some initial constraints on the age of groundwater samples in the region. Tritium is ideal for the dating of young groundwater (less than 60 years before present) because it is incorporated into water molecules and its activity is not affected by chemical or microbial processes, or by reactions between the groundwater and aquifer material (Stewart and Morgenstern, 2001). Electrolytic reduction was used to concentrate tritium in 500 ml of a water sample using a 20-cell standard Tritium Enrichment Unit. The temperature of the sample was maintained at 0° to 5°C to achieve maximum tritium fractionation and enrichment. After the electrolytic process, the sample volume was reduced to 25 ml. The tritium activity in enriched samples along with the standards was measured using an ultra-low-level liquid scintillation counter (Quantulus Wallac model 1220), and results are reported in tritium units (TU) with 2 sigma errors (Table S2).

4. Results

4.1. Oxygen and hydrogen isotopic composition of precipitation, surface water, and groundwater

4.1.1. Precipitation

Measured $\delta^{18}O$ and $\delta^{2}H$ values of precipitation from three sampling locations (Chandigarh, Patiala, and Sirsa) ranged between -14.8‰ and +5.8‰ for $\delta^{18}O$, and between -116.3‰ and +51.5‰ for $\delta^{2}H$ (Figure 2 & S1). The amount-weighted annual precipitation (AWAP) value of $\delta^{18}O$ was -6.5‰ and of $\delta^{2}H$ was -46.8‰. We checked the effect of altitude variation on isotopic values of precipitation from all three stations and this was found to be negligible. Remarkably enriched isotopic values were observed for rainfall events of less than 20 mm per day, particularly from the rain gauge station at Sirsa in the downstream part of the basin where the climate is semi-arid. A cross plot of $\delta^{18}O$ and $\delta^{2}H$ based on the monthly weighted isotopic composition of precipitation from all three sites was used to develop a Local Meteoric Water Line (LMWL) for the study area (Figure 2). This provides information on the preservation or alteration of the stable isotopic composition of groundwater and various other water sources. The LMWL derived for our study area, along with other LMWLs for the Delhi region and the Global Meteoric Water Line (GMWL), are as follows:

$\delta^2H = 7.9*\delta^{18}O + 5.56$, ($r^2 = 0.98$) [Study area] (1)

$\delta^2H = 7.15*\delta^{18}O + 2.60$, ($r^2$=0.98) [Delhi LMWL; Pang et al., 2004] (2)

$\delta^2H = 8.14(\pm0.02)*\delta^{18}O + 10.9(\pm0.2)$, ($r^2$=0.98) [GMWL; Gourcy et al., 2005] (3)

The slope of our LMWL (Eq. 1) is close to that of the GMWL (Eq. 3) defined by Gourcy et al. (2005) and the LMWL from Delhi (Eq. 2).

4.1.2. River and canal waters

The isotopic values of the Ghaggar River samples (*n=10*) varied from -7.5‰ to -6.7‰ for $\delta^{18}O$ and -54.9‰ and -43.8‰ for δ^2H. The $\delta^{18}O$ and δ^2H values of river water samples fall on the LMWL and in close proximity to the AWAP, indicating that modern local precipitation is the primary source of Ghaggar River water (Figure 3a). In contrast, Sutlej River water ranges from -12.6‰ to -10.5‰ for $\delta^{18}O$ and -87.8‰ to -70.9‰ for δ^2H. The $\delta^{18}O$ of canal water (*n=20*) varies from -12.0‰ to -10.6‰ while δ^2H ranges from -81.3‰ to -70.3‰ (Figure 3a, Table S1). The relative isotopic depletion of canal water compared to the Ghaggar River water and AWAP reflects the Higher Himalayan source of canal water that is derived from the Sutlej River.

4.1.3 Groundwater

The isotopic values of groundwater samples (*n=244*) varied between -11.6‰ and -4.7‰ for $\delta^{18}O$, and -81.4‰ and -34.5‰ for δ^2H (Figure 3a & b, Table S2). A cross plot of $\delta^{18}O$ and δ^2H of the groundwater samples is used to develop a groundwater regression line for the study area (Figure 3a, Table S2):

$$\delta^2H = 6.10*\delta^{18}O - 7.00, (r^2=0.95) \quad (4)$$

The clustering of a large number of groundwater samples around the LMWL indicates that local modern meteoric water is a significant source of groundwater recharge in the study area. However, a cluster of groundwater samples also falls below the GMWL. The slope and intercept of the groundwater regression line (Eq. 4) are less than those of the LMWL (Eq.1), indicating the important effect of evaporative enrichment on groundwater (Wassenaar et al., 2011).

Importantly, we observe systematic variations in $\delta^{18}O$ values of groundwater with relation to the depth from which the groundwater was sampled (Figures 4). Groundwater samples taken from depths in general above 80 mbgl show a broad range of $\delta^{18}O$ values (between -11.6‰ and -4.7‰,) and consistently lie very close to the AWAP and canal water samples (Figure 5c). These samples also show significant spatial variability in $\delta^{18}O$ values (Figure 5a). In contrast, samples from depths in general below 80 mbgl show a narrower range of values and located closely to the AWAP, varying between -8.2‰ and -4.8‰ for $\delta^{18}O$ and between -58.2‰ and -35.0‰ for δ^2H

(Figures 4, 5b & d). We define the regression lines for groundwater samples taken from both above and below 80 mbgl (Figure 3a & b) as follows:

$$\delta^2H = 6.10*\delta^{18}O - 7.14, (r^2 = 0.95) \text{ [groundwater samples above 80 mbgl]} \quad (5)$$

$$\delta^2H = 5.86*\delta^{18}O - 8.4, (r^2 = 0.97) \text{ [groundwater samples below 80 mbgl]} \quad (6)$$

Both regression lines (Eq. 5 & 6) have a lower slope than the GMWL and a negative intercept, suggesting evaporative enrichment of the groundwater.

4.2. Deuterium excess

The deuterium excess (d-excess) was defined as d = $\delta^2H - 8 \times \delta^{18}O$ (Dansgaard, 1964), and quantifies the surplus deuterium about Craig's line (Craig, 1961). The deuterium excess depends on conditions prevalent during primary evaporation, including variation in humidity, ocean surface temperature, and wind speed, and thus gives information on the sources of water vapour (Gat, 1983; Clark and Fritz 1997). While equilibrium processes do not change the d-excess for any of the phases, non-equilibrium evaporation causes a decrease in the d-excess which indicates an increase in the vapour phase. Most groundwater samples have d-excess values close to that of precipitation, and a few samples are similar to the d-excess value of canal water (Figure 6). The d-excess values of groundwater samples derived from depths in general above 80 mbgl are spatially variable and vary from -4.1‰ to +14.9‰ (Figures 8a), which depends upon the mixture of canal recharge or precipitation and groundwater irrigation return flow. In contrast, samples below 80 mbgl have d-excess values in the range of -

0.8 ‰ to +11.3 ‰, and most samples have values very close to that of precipitation (Figure 6). The negative and very low d-excess values of a few groundwater samples derived from below 80 m depth mainly correspond to the downstream part of the study area.

4.3. Tritium concentrations

Tritium concentration was measured for 91 samples of river, canal, and groundwater in the study area (Figure 7a, Table S3), and 22 samples of precipitation for Roorkee in north India (Table S4). The average tritium concentrations of precipitation and canal water samples were 8.2 ± 0.3 and 9.0 ± 0.3 TU, respectively. The tritium concentration in groundwater varies between ~0.1 TU (minimum) and 12.9 ± 0.5 TU (maximum). These values vary both vertically (i.e. with depth) and spatially (i.e. with distance from the Himalayan mountain front) (Figures 7b & c). Tritium concentration shows a clear decline with depth (Figure 7b), although groundwater samples taken generally above 80 mbgl show a much broader range of values, from 0.3 ± 0.2 up to 12.9 ± 0.5 TU, than samples from below that depth (Figure 7b & c). Spatially, Tritium concentrations vary from 1.3 ± 0.2 to 8.4 ± 0.4 TU particularly in the area within 80 km of the Himalayan front (Figure 7c). In the middle and downstream regions of the study area between 80 km and 320 km downstream of the Himalayan front (Figure 7c), TU values for samples from generally above 80 mbgl lie between 0.3 ± 0.2 to 10.2 ± 0.5. In contrast, tube well samples from generally below 80 mbgl show lower TU values, typically less than 4.4 ± 0.2. We observe three downstream patterns of TU value variation for those deeper samples, (Figures 7a & c): (1) In the area within 80 km of the Himalayan front, the majority of samples have TU values less than 1.2 ± 0.1 TU; (2) in the middle area between 80 to 200 km downstream, TU values vary from ~0.1 to 4.4 ± 0.2 TU; and (3) beyond 200 km downstream, TU values are less than 1.9 ± 0.2 TU (except for 3 measurements). Thus, the deeper samples generally show downstream TU variation compared to groundwater samples derived from in general above 80 mbgl.

4.4. Estimation of canal water contribution to groundwater recharge

The stable isotopic composition of groundwater samples from generally above 80 mbgl in a number of tube wells (especially in the middle and downstream parts of the basin) indicate important recharge from highly depleted canal water. We have quantified the proportion of this recharge using a two-component separation approach (Clark and Fritz., 1997; Rai et al., 2009; Engelhardt et al., 2014). For this, we assume that the isotopic composition of groundwater samples is derived by mixing of two end-member components, namely AWAP (average $\delta^{18}O$ value of -6.5 ‰) and canal water (-11.6 ‰). The volumetric ratio of canal recharge to total recharge, p, is then given by:

$$p = {(\delta^{18}O_{gw} - \delta^{18}O_{precip})}\Big/{(\delta^{18}O_{canal} - \delta^{18}O_{precip})} \qquad (8)$$

where $\delta^{18}O_{gw}$ is the value of groundwater, $\delta^{18}O_{precip}$ is the value of precipitation (AWAP), and $\delta^{18}O_{canal}$ is the average value of canal water.

The canal water contribution to groundwater recharge is spatially variable across the study area (Figure 8b). Most tube wells with depths of up to 80 mbgl in the downstream part of the basin have an estimated canal recharge component of more than 50% of total recharge, whereas this value is quite variable (25% to 50%) in the middle part of the basin.

5. Discussion

5.1. Spatial variation in isotopic characteristics of groundwater

Our analysis of isotopic characteristic of groundwater in the Ghaggar basin shows that $\delta^{18}O$ and $\delta^{2}H$) of groundwaters vary in space as well as depth. To understand the relationship between isotopic and aquifer characteristics, we have plotted aquifer thickness logs from the basin margin in Himalayan front to the distal part of the basin along cross-section A-B along with d-excess and isotopic composition ($\delta^{18}O$ and $\delta^{2}H$) of groundwaters (Figures 9a-e). The $\delta^{18}O$ values of groundwater samples range from -5.2 ‰ to -7.7 ‰, and from 1.2 to 8.4 TU for tritium concentration (generally above 80 mbgl) in the upstream parts (from the basin margin up to 80 km downstream, Figure 7c & 9d); these values clearly reflect that precipitation is the main recharge source. However, in the middle and downstream parts of the basin (~80 to 320 km downstream of the basin margin), the $\delta^{18}O$ value and tritium concentration of groundwater samples generally above 80 mbgl are much more variable than those from the generally below 80 mbgl. This could reflect multiple recharge sources such as irrigation return flow, canal water leakage, and precipitation in this part of the basin.

The cross-plot of d-excess vs. $\delta^{18}O$ for the groundwater samples shows an inverse correlation (Figure 6). The positive d-excess (>10‰) of the groundwater samples (generally above 80 mbgl) is consistent with source water derived from the Higher Himalayas (Pande et al., 2000; Rai et al., 2014) and provides additional evidence of recharge from Sutlej River water that has been redistributed through the canal network. A few samples have lower d-excess values, which suggests evaporative enrichment of groundwater during the recharge process. The d-excess values of groundwater samples that lie between canal water and AWAP values suggest mixing of groundwater from different sources. These d-excess results are broadly consistent with our $\delta^{18}O$ and $\delta^{2}H$ measurements. Low d-excess values in downstream part (between 280 and 320 km from the northern basin margin) suggest a significant evaporative enrichment of recharged groundwater (Figure 9c). This is likely due to the prevailing semi-arid climate in a southwest part of the study area and slow rate of recharge (56 mm/yr for Punjab and 70 mm/yr for Haryana; Rangarajan and Athavale, 2000). Towards the distal part of the basin, the thickness of non-aquifer material in the subsurface increases (van Dijk et al., 2016a). The spatial variation of $\delta^{18}O$ and $\delta^{2}H$ with distance suggests that *in-situ* vertical recharge at a variable rate takes place throughout the study area. This is obvious on account of the variable water table (Supplementary Figure S2) and heterogeneity in the subsurface in NWIA system (Figure 9a). The isotopic data is in conformity with the observed geological heterogeneity of the NWIA system and the decrease in bulk aquifer body percentage from proximal to distal parts of the basin, which results in limited lateral connectivity of aquifer bodies (van Dijk et al., 2016a, 2016b).

5.2. Vertical variability of $\delta^{18}O$ and tritium

Groundwater $\delta^{18}O$ values fall within a narrow range near the AWAP for samples generally below 80 mbgl (Figure 4). This is likely due to the attenuation of $\delta^{18}O$ and δ^2H values with depth, as water from different sources moves downward and attains the isotopic signature close to the AWAP generally below 80 mbgl (Figure 4). Similarly, a decrease in tritium concentration is observed with depth (Figure 7b). The comparatively low tritium concentrations below 80 mbgl indicate relatively large travel time in the groundwater flow system, resulting in loss of tritium by radioactive decay. As mentioned earlier, precipitation is the main recharge source, and therefore, we compare our results with tritium concentration of precipitation for the northwest India. The eight precipitation samples measured here yielded values of ~3 to 17 TU. Kumar et al. (2010) reported tritium concentrations of 6.6 to 17.6 TU for northwestern India, while tritium concentrations in precipitation measured during 2004 to 2010 at Roorkee in north India, varies between 2.6 and 15.5 TU (Table S4). We therefore consider tritium concentrations of groundwater of 2 to 12.9±0.5 TU as indicating recharge from modern water. However, tritium concentrations below 1 TU indicates groundwater that is likely older than 50 yrs (Liu et al., 2014). The presence of a mixture of modern and old water below 80 mbgl indicates that significant recharge from modern sources reaches down to tube well depth (i.e., 320 mbgl) except in a few locations. This, in turn, suggests that there is significant vertical leakage through the thick but discontinuous non-aquifer layers within the sedimentary sequence (van Dijk et al., 2016a) and that these layers do not provide a barrier to vertical recharge of groundwater (Bowen 1985, Toth, 2009;

Sinha et al., 2013; van Dijk et al., 2016a; Hoque et al., 2017: Figure 9b). Similar results have been reported by Lapworth et al. (2015) from the Beas-Sutlej region of Punjab using anthropogenic tracers.

5.3. Spatial variability in groundwater recharge sources and zones

The spatial variation of $\delta^{18}O$ values, tritium concentrations and d-excess of groundwater samples generally above 80 mbgl, and the canal contribution to groundwater recharge (Figures 5a, b, 7a, 8a & b) reveal spatially variable recharge processes in the study area. This leads us to identify four distinct groundwater recharge zones (Figure 8a).

Zone I represents the upstream area of the basin, where the d-excess ranges from +6‰ to +11‰ (Figure 8a). A cross-plot of $\delta^{18}O$ vs. $\delta^{2}H$ shows that all groundwater samples (generally above 80 mbgl) fall on the LMWL and are very close to AWAP (Figure 8c) suggesting recharge predominantly through local precipitation. Tritium concentrations in groundwater samples generally above 80 mbgl in this zone are up to 12.9 ± 0.5 TU. This indicates that the groundwater is of modern age, and derived from local meteoric precipitation. Previous work interpreted Zone I as characterized by high permeability and high hydraulic conductivity (van Dijk et al., 2016a). Our work, however, has shown that this zone is recharged by local precipitation based on the inferred groundwater recharge sources and flow paths. Therefore, the implication of our work is that recharge rates in this zone would be high although we do not provide any quantification at this stage.

Zone II represents an area where the d-excess ranges from +1‰ to +5‰ (Figure 8a) and groundwater samples fall on or below LMWL in the cross plot of $\delta^{18}O$ vs. $\delta^{2}H$ and very close to AWAP (Figure 8d). The primary source of recharge is local precipitation. However, a number of samples fall between the isotopic values of canal water and AWAP, indicating recharge through a mixture of canal water and local precipitation. The enriched isotopic composition and low d-excess of groundwater samples reflect fractionation during recharge through rainfall or irrigation return flow. Tritium concentrations of groundwater samples range from ~2 to ~10 TU, indicate modern recharge at depths generally above 80 mbgl. The canal contribution to groundwater in a number of locations, estimated by using two-component analysis, ranges from 0% to 50% in zone II (Figure 8b). This zone is characterized by a high tube well density and rapid decline in groundwater levels due to overexploitation of groundwater resources. Therefore, induced recharge to groundwater through irrigation return flow might be one explanation for evaporative enrichment of isotopic signatures of groundwater.

Zone III represents the area where the d-excess ranges from +8‰ to +15‰ (Figure 8a), and where $\delta^{18}O$ and $\delta^{2}H$ of the groundwater fall mostly above the LMWL and very close to the isotopic composition of canal water. Relatively more depleted values of $\delta^{18}O$ are observed in this zone compared with zones I and II, which we interpret as evidence of active recharge by canal water. Tritium values are also higher than those in zone II, because of the significant contribution of the canal to groundwater. The canal contribution to groundwater recharge ranges up to 100% (Figure 8b).

Zone IV represents the distal end of the study area where d-excess value ranges from -2‰ to +4‰, and $\delta^{18}O$ and $\delta^{2}H$ values fall below the LMWL but close to AWAP (Figure 8f). The $\delta^{18}O$ and $\delta^{2}H$ values of groundwater samples, more enriched than the AWAP, are evidence of recharge by local precipitation, modified by evaporative fractionation. This zone is characterized by semi-arid conditions. Here, water gets fractionated during the recharge process and bears enriched values of $\delta^{18}O$ and $\delta^{2}H$ and low d-excess. The canal contribution to groundwater at a number of locations, is less than 50% (Figure 8b). This is consistent with slow recharge rates in this zone (Rangarajan and Athavale, 2000).

5.4. Conceptual model of the hydrological processes controlling isotopic signatures of groundwater

It has already been established that the hydrological processes operating in the basin have subtle differences as we move downstream. Traced downstream, the variability in the recharge processes including the source and rate of recharge, appears to correlate with both the complex and spatially-variable subsurface sedimentary architecture (van Dijk et al., 2016a) and with anthropogenic forcing such as the canal network. We use this information to develop a conceptual model for the hydrological processes operating in the Ghaggar Basin (Figure 10). The boundary conditions for the conceptual model are: a) geomorphic setting, b) the spatial variability of $\delta^{18}O$ and $\delta^{2}H$, c) the spatial variation of tritium concentration in groundwater, d) longitudinal cross-sections based on aquifer-thickness logs, and e) groundwater flow directions derived from water table.

The available aquifer-thickness data, indicate that the aquifer system is composed of staked, laterally-discontinuous high-permeability aquifer bodies, separated both laterally and vertically by low-permeability non-aquifer material (Figure 9a). This interleaved pattern of occurrence, coupled with the basin surface topography, imposes and maintains a hierarchy of groundwater flow systems, from shallow to deep (Hoque et al., 2017). The flow systems can be referred as *local,* if recharge and discharge areas are contiguous; *intermediate,* if these regions are separated by one or more local systems; and *regional:* if they extend over the full extent of the basin (Toth, 2009). Our depth-wise isotopic data suggest that local flow patterns in the Ghaggar Basin extend down to a depth of c. 80 m and are dominated by local vertical recharge from meteoric and canal sources, while intermediate and regional flow patterns extend to deeper depths and show evidence for sustained lateral flow (Figure 10). A similar flow pattern has been proposed for the Bengal basin by Ravenscroft et al. (2005), and Toth (2009) showed similar hierarchically nested groundwater flow systems within the exploited depth of the aquifer. The observed vertical variations in isotopic signature of the groundwater are thus likely due to tortuous groundwater flow paths; surface topography and subsurface lithological variations impose hydraulic heterogeneity and anisotropy, which controls the flow patterns and depth of groundwater penetration (Zijl, 1999).

This conceptual model helps to explain the major lateral and vertical variations in groundwater $\delta^{18}O$, $\delta^{2}H$ and tritium concentrations, which we interpret as due to the heterogeneous distribution of aquifer and non-aquifer sediments in the subsurface. For example, the tritium results show comparatively higher residence time for groundwater from generally below 80 mbgl compared to the groundwater above 80 mbgl. This indicates the existence of longer flow paths for groundwater below 80 mbgl, which is likely controlled by the aquifer heterogeneity and anisotropy.

Furthermore, as illustrated in the schematic model in Figure 10, water recharged in zones I and II must travel deeper to account for the regional groundwater flow system. The groundwater velocity through sand-rich aquifer bodies like those in the Ghaggar Basin are typically ~1 to 2 m/day (Soni et. al., 2014; Shekhar, et. al., 2015). Furthermore, the model (Figure 10) suggests the hydrological process of mixing of this old groundwater in zone III with vertically recharged groundwater from sources like rainfall and return flow of canal and groundwater irrigation.

6. Conclusions

This study is the first systematic attempt to identify the recharge sources and zones and to characterise groundwater dynamics in the northwestern Indian aquifer in Punjab and Haryana using water isotopes ($\delta^{18}O$, $\delta^{2}H$ and ^{3}H). Our results reveal that recharge sources for groundwater in the region are local meteoric water, canal seepage, and both canal and groundwater-derived irrigation return flow. These recharge sources vary spatially in their importance. The influence of canal water to recharge is most apparent in the Zone II to IV in the study area. The spatial variability in $\delta^{18}O$, $\delta^{2}H$ value and tritium concentration reflects limited lateral connectivity of the aquifer due to the heterogeneity of aquifer material. However, the variation of $\delta^{18}O$ with depth shows the effect of averaging of the isotopic composition of different groundwater sources at various depths. Variability in tritium concentrations with depth reveals that groundwater generally above 80 mbgl is of modern age. However, groundwater generally below 80 mbgl is a mixture of modern and old water. The spatial distribution of aquifer and non-aquifer material in the subsurface likely forces some recharge water to follow longer, deeper, and more tortuous flow paths resulting in low tritium values. Two kinds of flow patterns are observed in the northwest Indian aquifer system: (i) a local flow pattern up to a general depth of c. 80 mbgl, and (ii) an intermediate and regional groundwater flow pattern in aquifer system generally below 80 mbgl, recharged with water from lateral groundwater flow and vertical infiltration. Results from this study can help in the identification of active recharge zones and for designing sustainable groundwater management strategies.

Acknowledgements

This project was supported by the Ministry of Earth Sciences, Government of India (Letter no.: MoES/NERC/16/02/10 PC-II) and the UK Natural Environment Research Council (grant NE/I022434/1) under the Changing Water Cycle program. We gratefully acknowledge Dr. Bhishm Kumar and Dr. Mohammad Hoque for insightful discussions. Constructive and positive reviews by Dr. Daren Gooddy and one anonymous reviewer helped to clarify and strengthen the manuscript. We are also thankful to Er. R. D. Singh, Director National Institute of Hydrology, Roorkee, for providing generous help to conduct this study. This work forms a part of the PhD thesis of Mr. Suneel Kumar Joshi and facilities used at IIT Kanpur for this work are thankfully acknowledged.

References

Aeschbach-Hertig, W. and Gleeson, T., 2012. Regional strategies for the accelerating global problem of groundwater depletion. Nature Geoscience 5(12), 853-861.

Ambast, S., Tyagi, N. and Raul, S., 2006. Management of declining groundwater in the Trans Indo-Gangetic Plain (India): some options. Agricultural Water Management 82(3), 279-296.

Bhadra, B.K., Gupta, A.K. and Sharma, J.R., 2009. Saraswati Nadi in Haryana and its linkage with the Vedic Saraswati River - Integrated study based on satellite images and ground-based information. Journal of the Geological Society of India 73(2), 273-288.

Bowen, R., 1985. Hydrogeology of the Bist Doab and adjacent areas, Punjab, India. Hydrology Research 16(1), 33-44.

Brenninkmeijer, C. and Morrison, P., 1987. An automated system for isotopic equilibration of CO_2 and H_2O for ^{18}O analysis of water. Chemical Geology: Isotope Geoscience section 66(1), 21-26.

Cardenas, M.B. and Jiang, X.W., 2010. Groundwater flow, transport, and residence times through topography-driven basins with exponentially decreasing permeability and porosity. Water Resources Research 46(11).

CGWB, 2009. Bhu-Jal news Central Ground Water Board.

CGWB, 2012. Report on Geophysical studies in Punjab State. June (Eds), Central Ground Water Board, North Western Region, Chandigarh.

Chen, J., Li, J., Zhang, Z. and Ni, S., 2014. Long-term groundwater variations in Northwest India from satellite gravity measurements. Global and Planetary Change 116, 130-138.

Clark, I.D. and Fritz, P., 1997. Environmental isotopes in hydrogeology, CRC press.

Craig, H., 1961. Isotopic variations in meteoric waters. Science 133(3465), 1702-1703.

Dansgaard, W., 1964. Stable isotopes in precipitation. Tellus A 16(4).

Datta, P.S., Bhattacharya, S.K. and Tyagi, S.K., 1996. ^{18}O studies on recharge of phreatic aquifers and groundwater flow-paths of mixing in the Delhi area. Journal of Hydrology 176(1–4), 25-36.

Dincer, T., Payne, B., Florkowski, T., Martinec, J. and Tongiorgi, E., 1970. Snowmelt runoff from measurements of tritium and oxygen-18. Water Resources Research 6(1), 110-124.

Döll, P., Hoffmann-Dobrev, H., Portmann, F.T., Siebert, S., Eicker, A., Rodell, M., Strassberg, G. and Scanlon, B., 2012. Impact of water withdrawals from groundwater and surface water on continental water storage variations. Journal of Geodynamics 59, 143-156.

Engelhardt, I., Barth, J., Bol, R., Schulz, M., Ternes, T., Schüth, C. and van Geldern, R., 2014. Quantification of long-term wastewater fluxes at the surface water/groundwater-interface: an integrative model perspective using stable isotopes and acesulfame. Science of the Total Environment 466, 16-25.

Epstein, S. and Mayeda, T., 1953. Variations of the 18O/16O ratio in natural waters. Geochim. Cosmochim. Acta 4, 213-224.

Fishman, R.M., Siegfried, T., Raj, P., Modi, V. and Lall, U., 2011. Over-extraction from shallow bedrock versus deep alluvial aquifers: Reliability versus sustainability considerations for India's groundwater irrigation. Water Resources Research 47(6).

Fontes, J.C., 1980. Handbook of environmental isotope geochemistry. Vol. 1.

Foster, S. and Chilton, P., 2003. Groundwater: the processes and global significance of aquifer degradation. Philosophical Transactions of the Royal Society of London B: Biological Sciences 358(1440), 1957-1972.

Gassiat, C., Gleeson, T. and Luijendijk, E., 2013. The location of old groundwater in hydrogeologic basins and layered aquifer systems. Geophysical Research Letters 40(12), 3042-3047.

Gat, J.R., 1983. Palaeoclimates and Palaeowaters: A Collection of Environmental Isotope Studies: Proceedings of an Advisory Group Meeting on the Variations of the Isotopic Composition of Precipitation and of Groundwater During the Quaternary as a Consequence of Climatic Changes, IAEA.

Gleeson, T., Befus, K.M., Jasechko, S., Luijendijk, E. and Cardenas, M.B., 2015. The global volume and distribution of modern groundwater. Nature Geoscience 9(2), 161-167.

Gourcy, L.L., Groening, P.K., Aggarwal, P.K., 2005. Stable oxygen and hydrogen isotopes in precipitation. In: Aggarwal, P.K., Gat, J.R., Froehlich, K.F.O. (Eds). Isotopes in the Water Cycle: Past, Present and Future of a Developing Science, pp.39-51

Hoque, M.A. and Burgess, W.G., 2012. ^{14}C dating of deep groundwater in the Bengal Aquifer System, Bangladesh: implications for aquifer anisotropy, recharge sources and sustainability. Journal of Hydrology, 444, pp.209-220.

Hoque, M., Burgess, W. and Ahmed, K., 2017. Integration of aquifer geology, groundwater flow and arsenic distribution in deltaic aquifers-a unifying concept. Hydrological processes.

Kazemi, G.A., Lehr, J.H. and Perrochet, P., 2006. Groundwater age. John Wiley & Sons.

Konikow, L.F. and Kendy, E., 2005. Groundwater depletion: A global problem. Hydrogeology Journal 13(1), 317-320.

Kulkarni, K.M., Navada, S.V., Rao, S.M., Nair, A.R., Kulkarni, U.P. and Sharma, S., 1996. Effect of the Holocene climate on composition of groundwater in parts of Haryana, India: Isotopic evidence Isotopes in Water Resources Management, International Atomic Energy Agency, Vienna (Austria), 2(Proceedings Series), 439-454.

Kumar, R., Singh, K., Singh, B. and Aulakh, S.S., 2014. Mapping groundwater quality for irrigation in Punjab, North-West India, using geographical information system. Environmental Earth Sciences 71(1), 147-161.

Kumar, R., Singh, R. and Sharma, K., 2005. Water resources of India. Current Science 89(5), 794-811.

Kumar, U.S., Kumar, B., Rai, S.P. and Sharma, S., 2010. Stable isotope ratios in precipitation and their relationship with meteorological conditions in the Kumaon Himalayas, India. Journal of Hydrology, 391(1), pp.1-8.

Lapworth, D., Krishan, G., MacDonald, A. and Rao, M., 2017. Groundwater quality in the alluvial aquifer system of northwest India: New evidence of the extent of anthropogenic and geogenic contamination. Science of the Total Environment 599, 1433-1444.

Lapworth, D.J., MacDonald, A.M., Krishan, G., Rao, M.S., Gooddy, D.C. and Darling, W.G., 2015. Groundwater recharge and age-depth profiles of intensively exploited groundwater resources in northwest India. Geophysical Research Letters.

Long, D., Chen, X., Scanlon, B.R., Wada, Y., Hong, Y., Singh, V.P., Chen, Y., Wang, C., Han, Z. and Yang, W., 2016. Have GRACE satellites overestimated groundwater depletion in the Northwest India Aquifer? Scientific reports 6.

Lorenzen, G., Sprenger, C., Baudron, P., Gupta, D. and Pekdeger, A., 2012. Origin and dynamics of groundwater salinity in the alluvial plains of western Delhi and adjacent territories of Haryana State, India. Hydrological Processes 26(15), 2333-2345.

Liu, J., Chen, Z., Wei, W., Zhang, Y., Li, Z., Liu, F. and Guo, H., 2014. Using chlorofluorocarbons (CFCs) and tritium (^3H) to estimate groundwater age and flow velocity in Hohhot Basin, China. Hydrological Processes, 28(3), pp.1372-1382.

Panda, D.K. and Wahr, J., 2015. Spatiotemporal evolution of water storage changes in India from the updated GRACE-derived gravity records. Water Resources Research 52(1), 135-149.

Pande, K., Padia, J., Ramesh, R. and Sharma, K., 2000. Stable isotope systematics of surface water bodies in the Himalayan and Trans-Himalayan (Kashmir) region. Journal of Earth System Science 109(1), 109-115.

Pang, H., He, Y., Zhang, Z., Lu, A. and Gu, J., 2004. The origin of summer monsoon rainfall at New Delhi by deuterium excess. Hydrology and Earth System Sciences Discussions 8(1), 115-118.

Rai, S., Kumar, B. and Singh, P., 2009. Bhagirathi River near Gaumukh, western Himalayas, India, using oxygen-18 isotope. Current Science 97(2), 240.

Rai, S., Purushothaman, P., Kumar, B., Jacob, N. and Rawat, Y., 2014. Stable isotopic composition of precipitation in the River Bhagirathi Basin and identification of source vapour. Environmental Earth Sciences 71(11), 4835-4847.

Rangarajan, R. and Athavale, R., 2000. Annual replenishable ground water potential of India - an estimate based on injected tritium studies. Journal of Hydrology 234(1), 38-53.

Rao, M., Krishan, G., Kumar, C., Purushothaman, P. and Kumar, S., 2017. Observing changes in groundwater resource using hydrochemical and isotopic parameters: a case study from Bist Doab, Punjab. Environmental Earth Sciences 76(4), 175.

Ravenscroft, P., Burgess, W.G., Ahmed, K.M., Burren, M. and Perrin, J., 2005. Arsenic in groundwater of the Bengal Basin, Bangladesh: Distribution, field relations, and hydrogeological setting. Hydrogeology Journal 13(5-6), 727-751.

Rodell, M., Velicogna, I. and Famiglietti, J.S., 2009. Satellite-based estimates of groundwater depletion in India. Nature 460(7258), 999-1002.

Saini, H.S., Tandon, S.K., Mujtaba, S., Pant, N.C. and Khorana, R.K., 2009. Reconstruction of buried channel-floodplain systems of the northwestern Haryana Plains and their relation to the 'Vedic' Saraswati. Current Science 97(11), 1634-1643.

Shekhar, S., Mao, R.S. and Imchen, E.B., 2015. Groundwater management options in North district of Delhi, India: A groundwater surplus region in over-exploited aquifers. Journal of Hydrology: Regional Studies 4, 212-226.

Singh, A., Thomsen, K.J., Sinha, R., Buylaert, J.P., Carter, A., Mark, D.F., Mason, P.J., Densmore, A.L., Murray, A.S., Jain, M. and Paul, D., 2017. Counter-intuitive influence of Himalayan river morphodynamics on Indus Civilisation urban settlements. Nature communications, 8(1), p.1617.

Sinha, R., Yadav, G., Gupta, S., Singh, A. and Lahiri, S., 2013. Geo-electric resistivity evidence for subsurface palaeochannel systems adjacent to Harappan sites in northwest India. Quaternary International 308, 66-75.

Soni, V., Shekhar, S. and Singh, D., 2014. Environmental flow for the Yamuna river in Delhi as an example of monsoon rivers in India. Current Science 106(4), 558-564.

Stewart, M. and Morgenstern U., 2001. Age and Source of groundwater from Isotope Tracers. *In* Groundwaters of New Zealand, M.R. Rosen and P.A. White (eds.). New Zealand Hydrological Society Inc., Wellington. P161-183.

Tiwari, V.M., Wahr, J. and Swenson, S., 2009. Dwindling groundwater resources in northern India, from satellite gravity observations. Geophysical Research Letters 36(18).

Tóth, J., 2009. Gravitational systems of groundwater flow: theory, evaluation, utilization, Cambridge University Press.

UNDP, 1985. Groundwater studies in the Ghaggar river basin in Punjab, Haryana and Rajasthan, United Nation Development Programme.

van Dijk, W.M., Densmore, A., Singh, A., Gupta, S., Sinha, R., Mason, P., Joshi, S., Nayak, N., Kumar, M. and Shekhar, S., 2016a. Linking the morphology of fluvial fan systems to aquifer stratigraphy in the Sutlej-Yamuna plain of northwest India. Journal of Geophysical Research: Earth Surface.

van Dijk, W.M., Densmore, A.L., Sinha, R., Singh, A. and Voller, V.R., 2016b. Reduced-complexity probabilistic reconstruction of alluvial aquifer stratigraphy, and application to sedimentary fans in northwestern India. Journal of Hydrology, 541, pp.1241-1257.

Wada, Y., van Beek, L.P.H. and Bierkens, M.F.P., 2012. Nonsustainable groundwater sustaining irrigation: A global assessment. Water Resources Research 48(6).

Wassenaar, L., Athanasopoulos, P. and Hendry, M., 2011. Isotope hydrology of precipitation, surface and ground waters in the Okanagan Valley, British Columbia, Canada. Journal of Hydrology 411(1), 37-48.

Zijl, W., 1999. Scale aspects of groundwater flow and transport systems. Hydrogeology Journal 7(1), 139-150.

Figure 1. Geomorphic map of the study area, modified after van Dijk et al. (2016a). The continuous blue lines represents surface rivers. The continuous orange lines represent the canal network. Three rain gauges were installed at Sirsa, Patiala and Chandigarh (green squares) to collect precipitation samples. Canal water sampling locations are shown by red triangles, river water samples by yellow squares, and groundwater samples by grey circles. Basin margin sampling point is shown as a black square.

Figure 2. Cross plot of $\delta^{18}O$ and $\delta^{2}H$ for precipitation samples (grey open squares); solid black line shows the LMWL and grey solid line shows the GMWL, big triangle shows the value of Amount Weighted Annual Precipitation (AWAP).

Figure 3. (a) Cross plot of $\delta^{18}O$ and $\delta^{2}H$ for groundwater samples (generally above 80 mbgl shown by purple circles, and generally below 80 mbgl shown by orange circles) along with canal samples (red triangles), Ghaggar River samples (yellow squares), and Sutlej River samples (blue squares). Black continuous line represents the local meteoric water line (LMWL), grey continuous line shows the global meteoric water line (GMWL), and black dashed line is the groundwater (GW) regression line. (b) Cross plot of $\delta^{18}O$ and $\delta^{2}H$ for groundwater samples generally above and below 80 mbgl, indicating different recharge conditions in the Ghaggar basin in northwestern Indian aquifer system.

Figure 4. $\delta^{18}O$ variation with sampling depth for all groundwater samples within the study area. The distinction between samples taken generally above 80 mbgl are wider

in range, which shows the multiple sources of recharge up to the depth of 80 m compared to samples below that depth.

Figure 5. (a) and (b) show spatial variation of $\delta^{18}O$ values for groundwater samples taken generally above and below 80 mbgl, respectively. The continuous blue lines represent river network. Basin margin point is shown by black square. The Ghaggar basin boundary shown by red continuous line, and the administrative boundary between Punjab and Haryana is shown by the grey continuous line. Panels (c) and (d) show cross plot of $\delta^{18}O$ and $\delta^{2}H$ for groundwater samples from two different depth zones - above 80 mbgl (purple circles) and below 80 mbgl (orange circles). Red triangles represent canal water samples, yellow squares are Ghaggar River water samples, and blue squares are Sutlej River water samples. Black continuous line is the LMWL and the grey continuous line is GMWL.

Figure 6. Cross plot of $\delta^{18}O$ values and d-excess. Groundwater samples are represented by purple circles (above 80 mbgl) and orange circles (below 80 mbgl). Red triangles represent canal water samples, yellow squares are Ghaggar River water samples, and blue squares are Sutlej River water samples.

Figure 7. (a) Spatial distribution of tritium concentrations in groundwater samples (generally above and below 80 mbgl) in the Ghaggar River basin. The continuous blue lines represent river network. Basin margin point is shown by black square. The Ghaggar basin boundary shown by red continuous line, and the administrative boundary

between Punjab and Haryana is shown by the grey continuous line. (b) Variation of tritium concentrations with depth of groundwater samples represented by purple circles (above 80 mbgl) and orange circles (below 80 mbgl), and (c) Tritium concentration as a function of distance from the basin margin from the Himalayan front.

Figure 8. (a) Spatial variation of d-excess of groundwater samples generally above 80 mbgl. There are four distinct zones, I to IV, shown by black dashed line, indicating different recharge sources for the study area. (b) Spatial variation of canal contribution to the groundwater recharge in the study area derived from the two-component mixing model. Panels (c) - (f) show cross plots of δ^2H and $\delta^{18}O$ of groundwater samples generally above 80 mbgl (purple circles), where d-excess varies between 6‰ and 11‰ in zone I, between 1‰ and 5‰ in zone II, between 8‰ and 15‰ in zone III, and between -2‰ and 4‰ in zone IV.

Figure 9. (a) Cross section A-B (see Figure 1 for location) showing Central Groundwater Board aquifer-thickness logs from the study area, modified from van Dijk et al. (2016a). Depth ranges with non-aquifer material are colored green and ranges with aquifer material are colored yellow. Note that aquifer bodies cannot be correlated laterally with the available data; median log spacing is 7 km. (b) the geographic location of point A and B, which is used to prepare cross section A-B, basin margin point in black color filled-square and Ghaggar River basin. (c) Downstream variation of d-excess with distance from the basin margin from the Himalayan front. (d) Downstream variation of

$\delta^{18}O$ values from the basin margin from the Himalayan front. (e) Downstream variation of $\delta^{2}H$ values from the basin margin from the Himalayan front.

Figure 10. Schematic model of the hydrological processes in the groundwater system of the Ghaggar River basin in northwestern Indian Aquifer system. The Sutlej and Yamuna sediments fans indicate thinning of the aquifer material from proximal to distal margin. The schematic model is categorised into four zones (Figure 8a), zone I and II are very close to the proximal part of the basin where rainfall amount varies from 800 to 1200 mm / year, indicating precipitation is the main recharge source in both zones I and II. Further, recharged water travel deeper and join the regional groundwater flow system in zones I and II. The depleted isotopic value in zone III indicates active recharge source from higher altitude and mixing between groundwater and surface water. The enriched isotopic value in zone IV (located in semi-arid condition where rainfall amount is less than 400 mm/year) indicates evaporative enrichment due to the less aquifer material in the distal margin of Sutlej and Yamuna sediments fans in northwest Indian aquifer system.

Figure

Figure 1

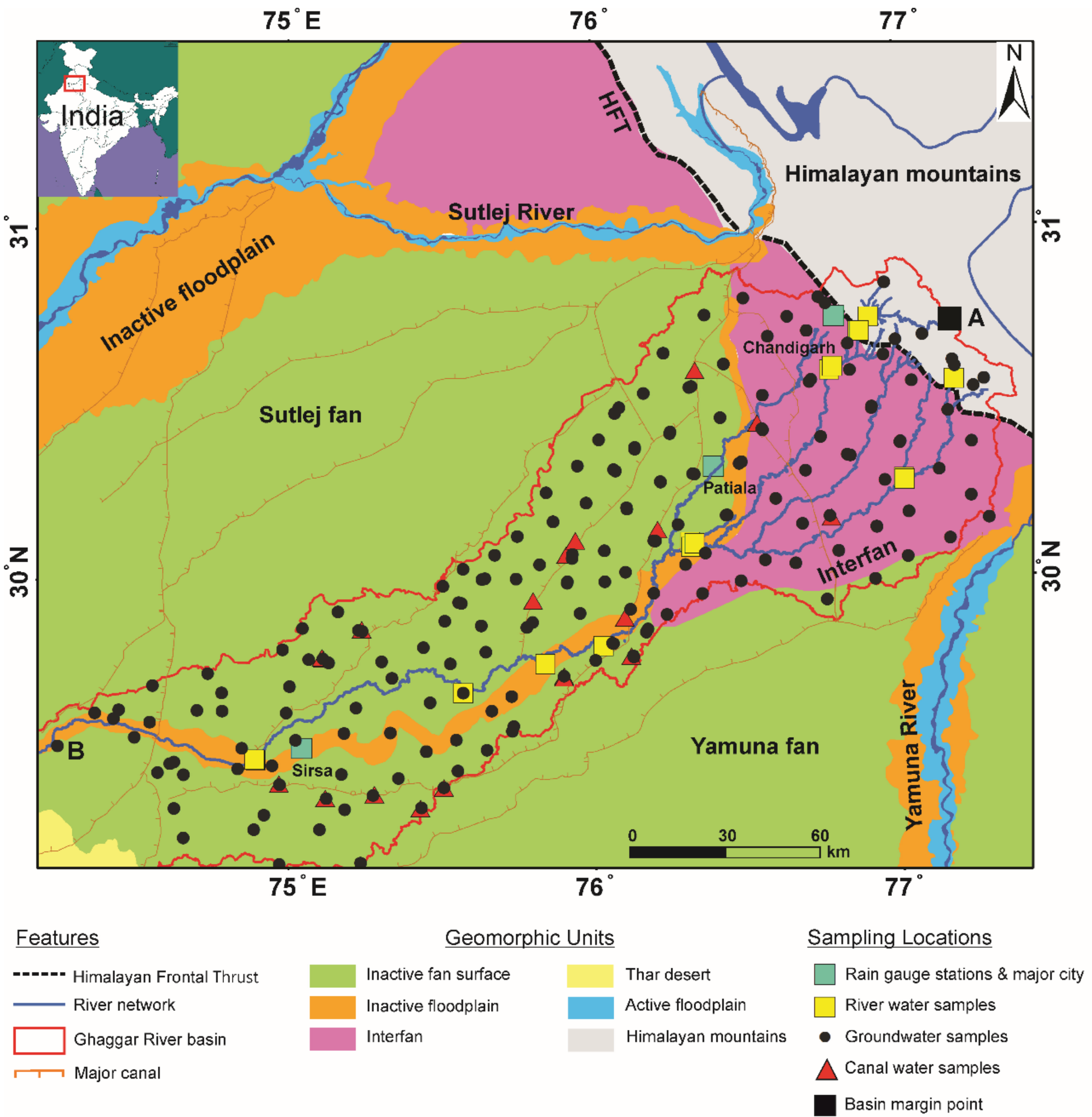

Figure 2

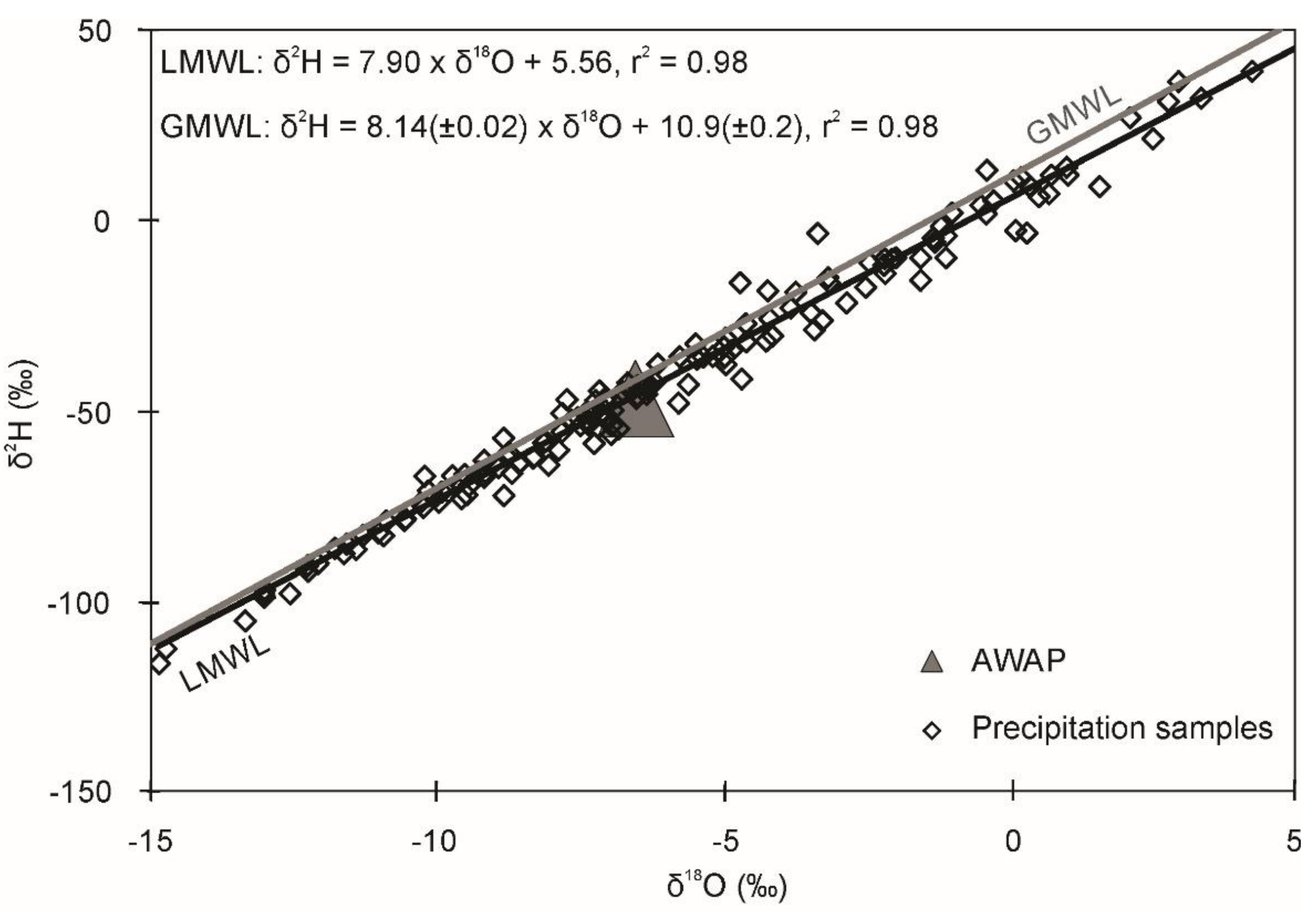

LMWL: δ²H = 7.90 x δ¹⁸O + 5.56, r² = 0.98
GMWL: δ²H = 8.14(±0.02) x δ¹⁸O + 10.9(±0.2), r² = 0.98
GMWL
LMWL
AWAP
Precipitation samples
δ²H (‰)
δ¹⁸O (‰)
50
0
-50
-100
-150
-15
-10
-5
0
5

Figure 3

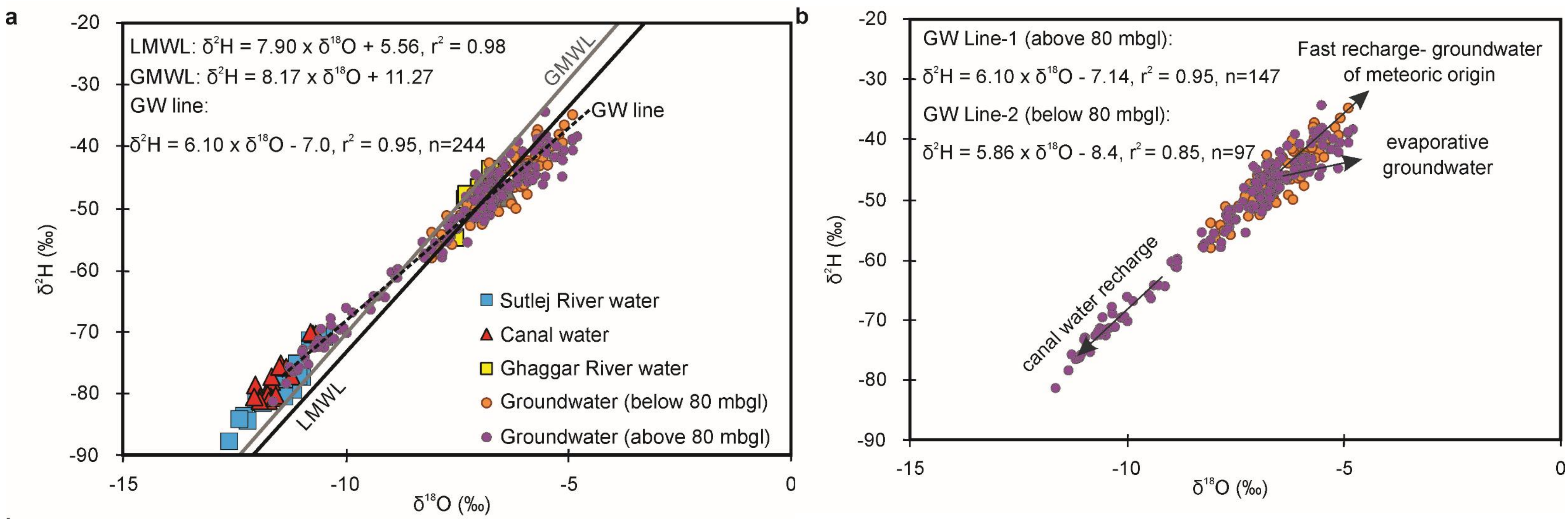

a
LMWL: δ²H = 7.90 x δ¹⁸O + 5.56, r² = 0.98
GMWL: δ²H = 8.17 x δ¹⁸O + 11.27
GW line:
δ²H = 6.10 x δ¹⁸O - 7.0, r² = 0.95, n=244
GMWL
GW line
LMWL
Sutlej River water
Canal water
Ghaggar River water
Groundwater (below 80 mbgl)
Groundwater (above 80 mbgl)
δ²H (‰)
δ¹⁸O (‰)
-20
-30
-40
-50
-60
-70
-80
-90
-15
-10
-5
0
b
GW Line-1 (above 80 mbgl):
δ²H = 6.10 x δ¹⁸O - 7.14, r² = 0.95, n=147
GW Line-2 (below 80 mbgl):
δ²H = 5.86 x δ¹⁸O - 8.4, r² = 0.85, n=97
Fast recharge- groundwater of meteoric origin
evaporative groundwater
canal water recharge
δ²H (‰)
δ¹⁸O (‰)
-20
-30
-40
-50
-60
-70
-80
-90
-15
-10
-5
0

Figure 4

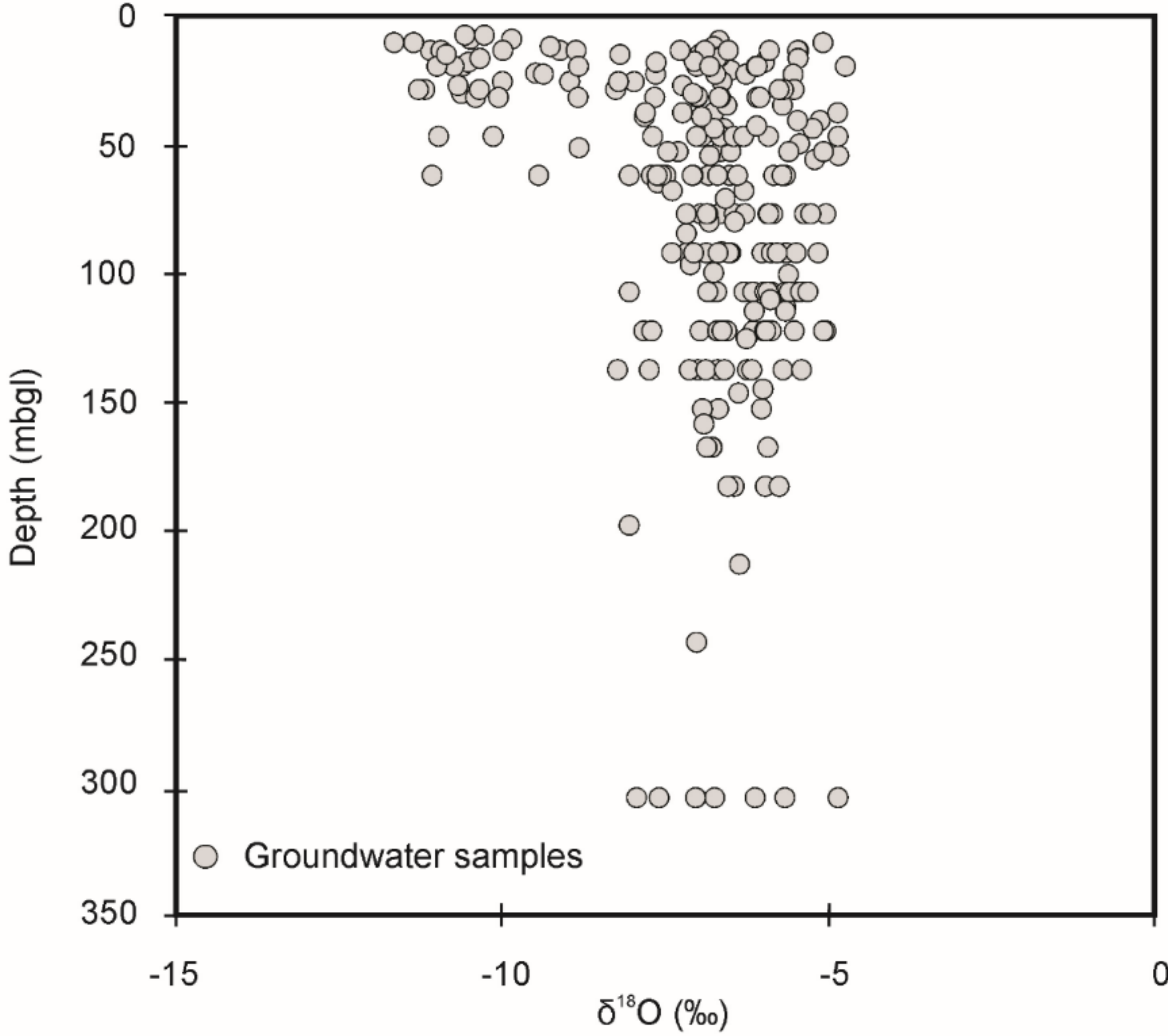

0
50
100
150
200
250
300
350
Depth (mbgl)
-15
-10
-5
0
δ18O (‰)
Groundwater samples

Figure 5

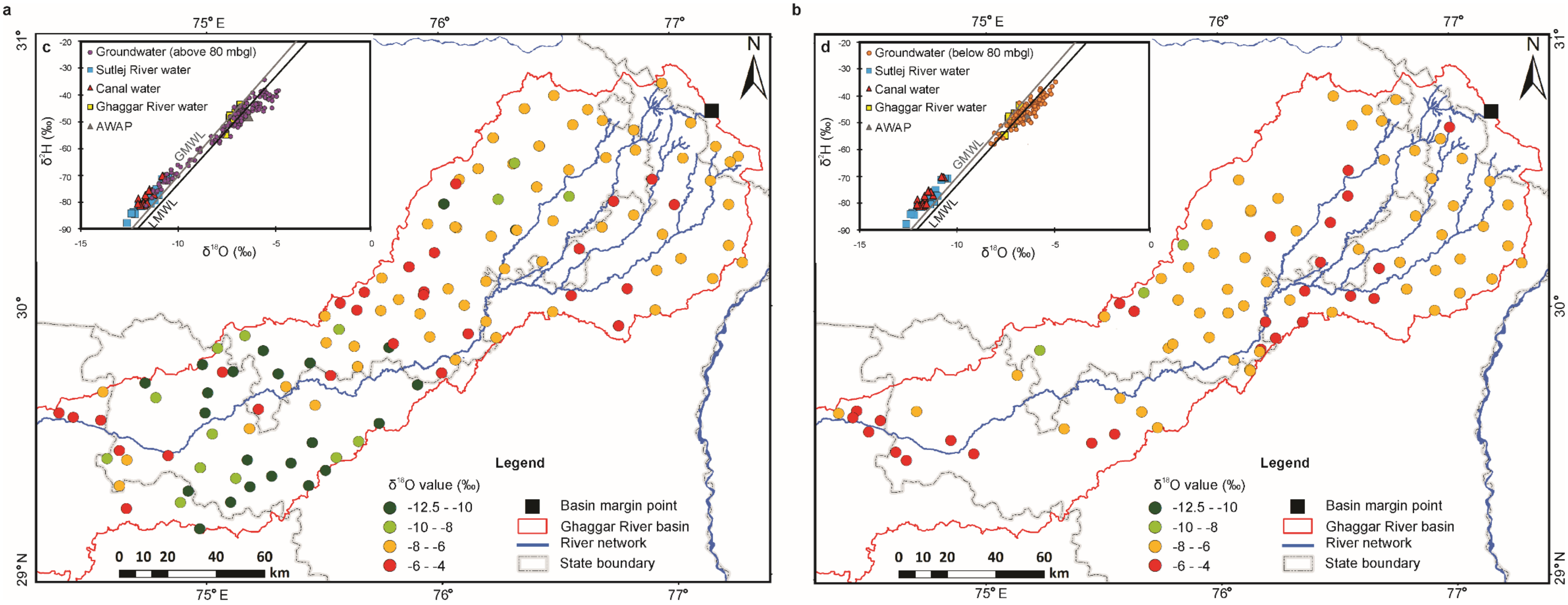
a
b
c
d
75° E
76°
77°
31°
30°
29° N
N
Groundwater (above 80 mbgl)
Groundwater (below 80 mbgl)
Sutlej River water
Canal water
Ghaggar River water
AWAP
GMWL
LMWL
δ²H (‰)
δ¹⁸O (‰)
Legend
δ¹⁸O value (‰)
-12.5 - -10
-10 - -8
-8 - -6
-6 - -4
Basin margin point
Ghaggar River basin
River network
State boundary
0 10 20 40 60 km

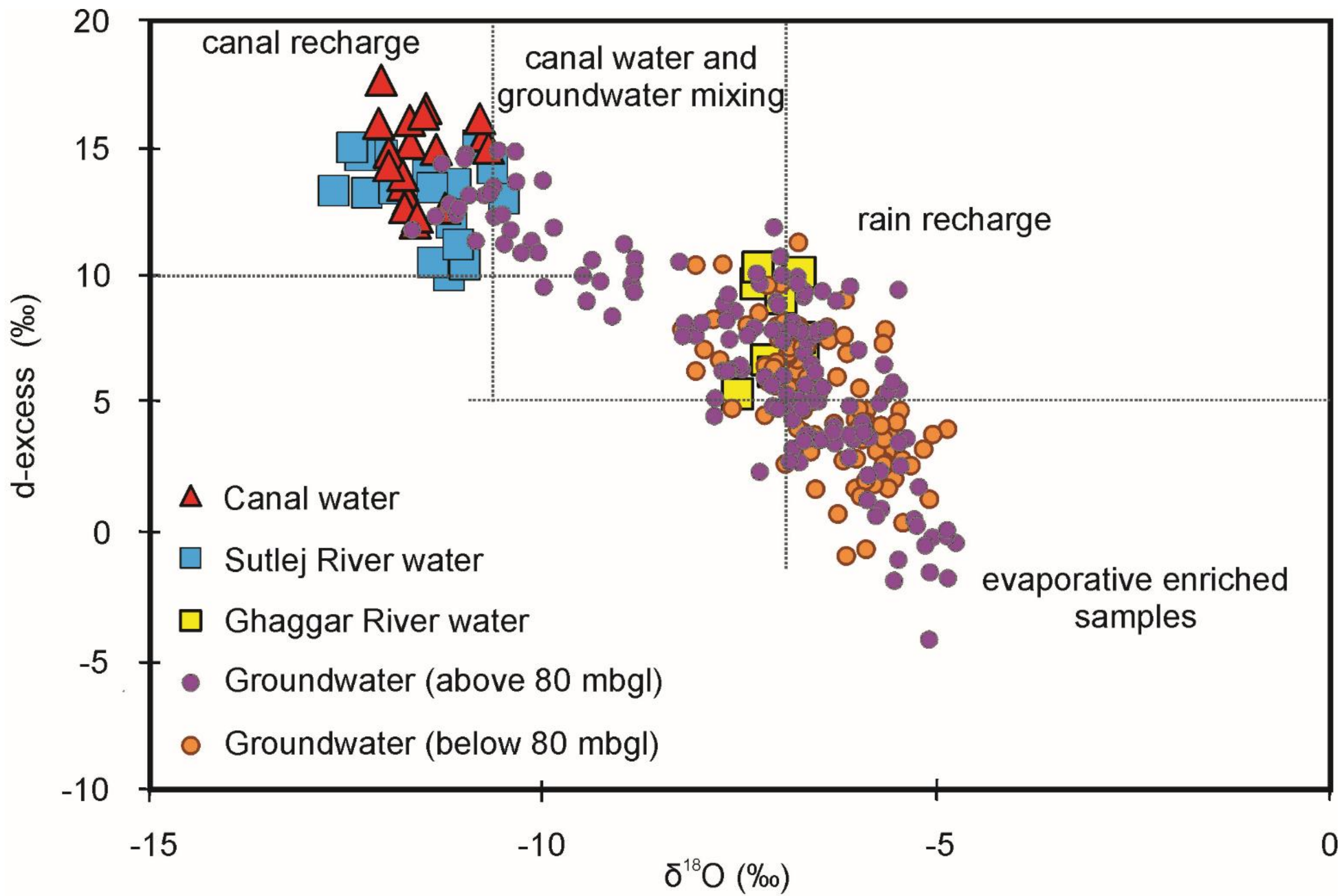
canal recharge
canal water and
groundwater mixing
rain recharge
evaporative enriched
samples
Canal water
Sutlej River water
Ghaggar River water
Groundwater (above 80 mbgl)
Groundwater (below 80 mbgl)
d-excess (‰)
δ18O (‰)
20
15
10
5
0
-5
-10
-15
-10
-5
0

Figure 6

Figure 7

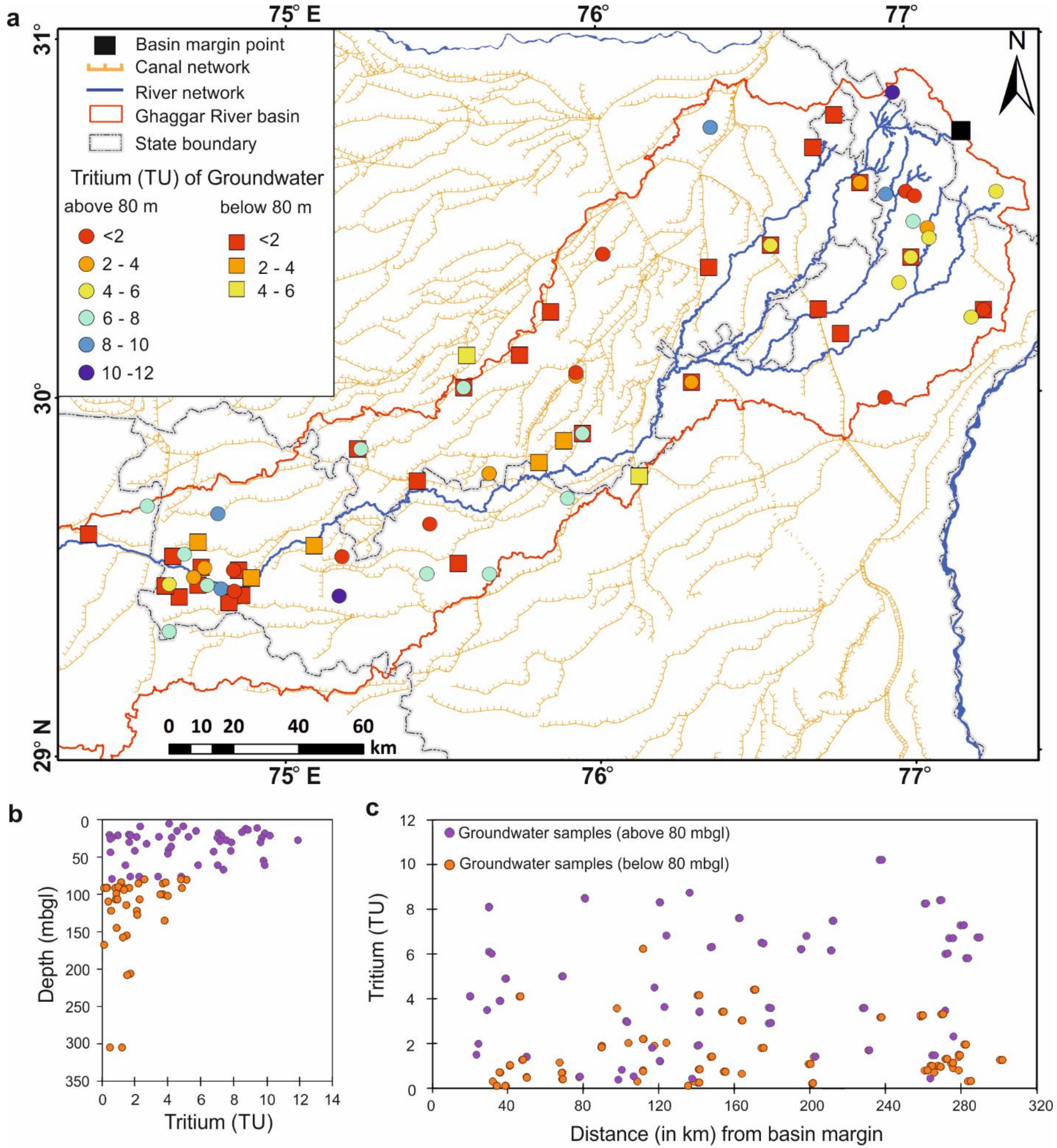

a
75° E
76°
77°
31°
30°
29° N
N
Basin margin point
Canal network
River network
Ghaggar River basin
State boundary
Tritium (TU) of Groundwater
above 80 m
below 80 m
<2
2 - 4
4 - 6
6 - 8
8 - 10
10 -12
0 10 20 40 60
km
b
Depth (mbgl)
Tritium (TU)
c
Groundwater samples (above 80 mbgl)
Groundwater samples (below 80 mbgl)
Tritium (TU)
Distance (in km) from basin margin

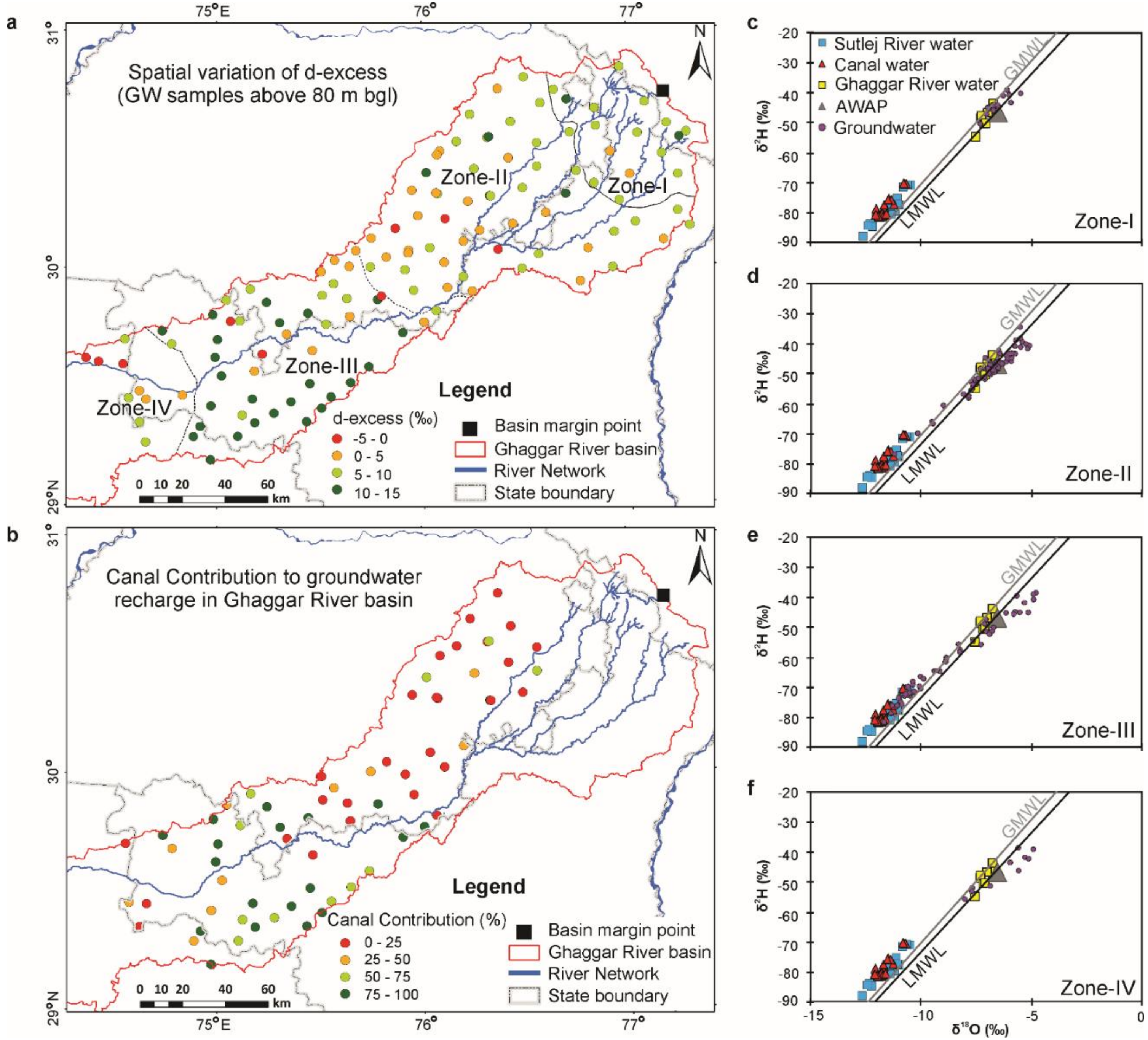

a
Spatial variation of d-excess
(GW samples above 80 m bgl)
Zone-I
Zone-II
Zone-III
Zone-IV
Legend
d-excess (‰)
-5 - 0
0 - 5
5 - 10
10 - 15
Basin margin point
Ghaggar River basin
River Network
State boundary
b
Canal Contribution to groundwater
recharge in Ghaggar River basin
Legend
Canal Contribution (%)
0 - 25
25 - 50
50 - 75
75 - 100
75°E
76°
77°
31°
30°
29°N
0 10 20 40 60 km
c
d
e
f
Sutlej River water
Canal water
Ghaggar River water
AWAP
Groundwater
GMWL
LMWL
δ²H (‰)
δ¹⁸O (‰)
Zone-I
Zone-II
Zone-III
Zone-IV

Figure 8

Figure 9

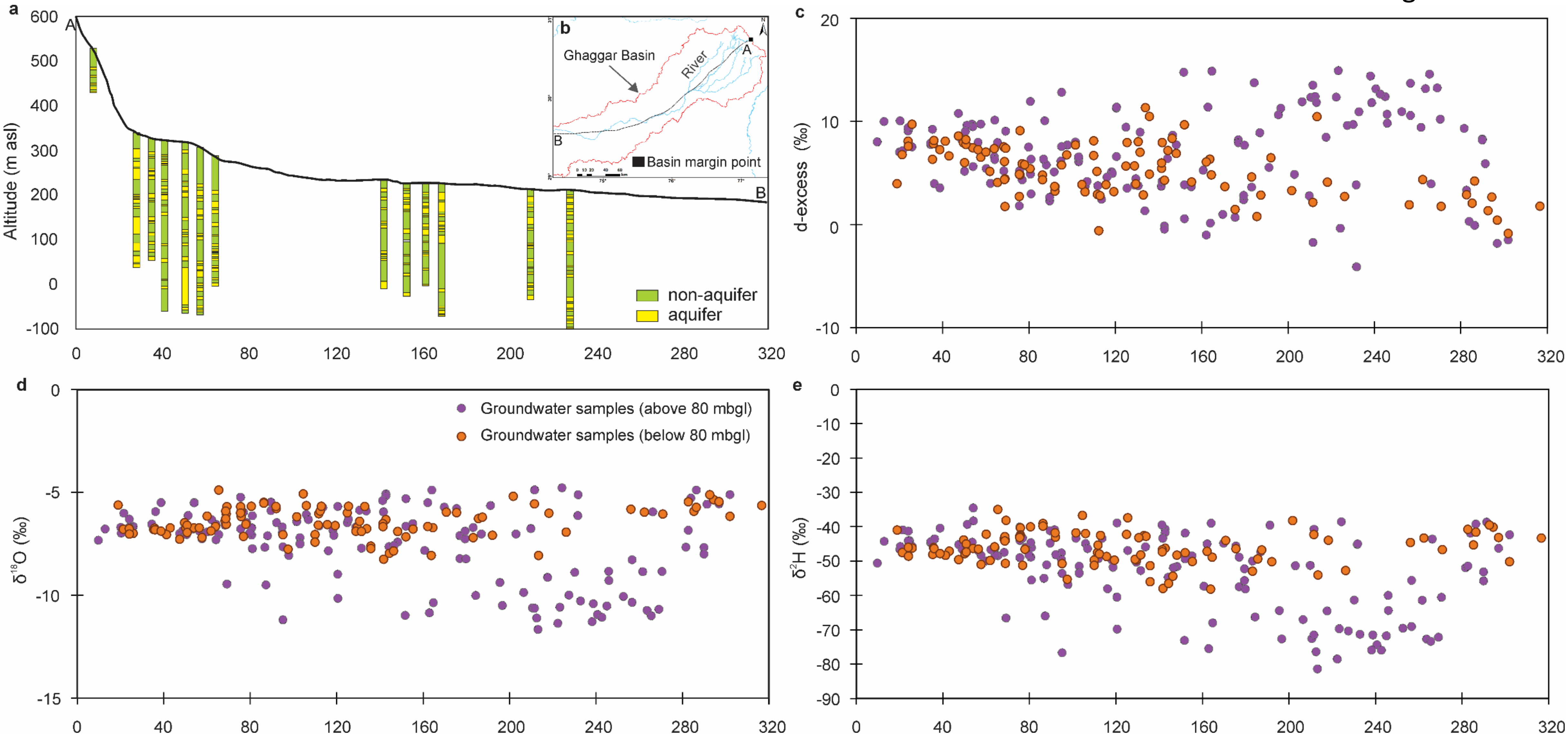

a
A
B
Altitude (m asl)
non-aquifer
aquifer
b
Ghaggar Basin
River
Basin margin point
c
d-excess (‰)
d
$\delta^{18}O$ (‰)
Groundwater samples (above 80 mbgl)
Groundwater samples (below 80 mbgl)
e
$\delta^{2}H$ (‰)

Figure 10

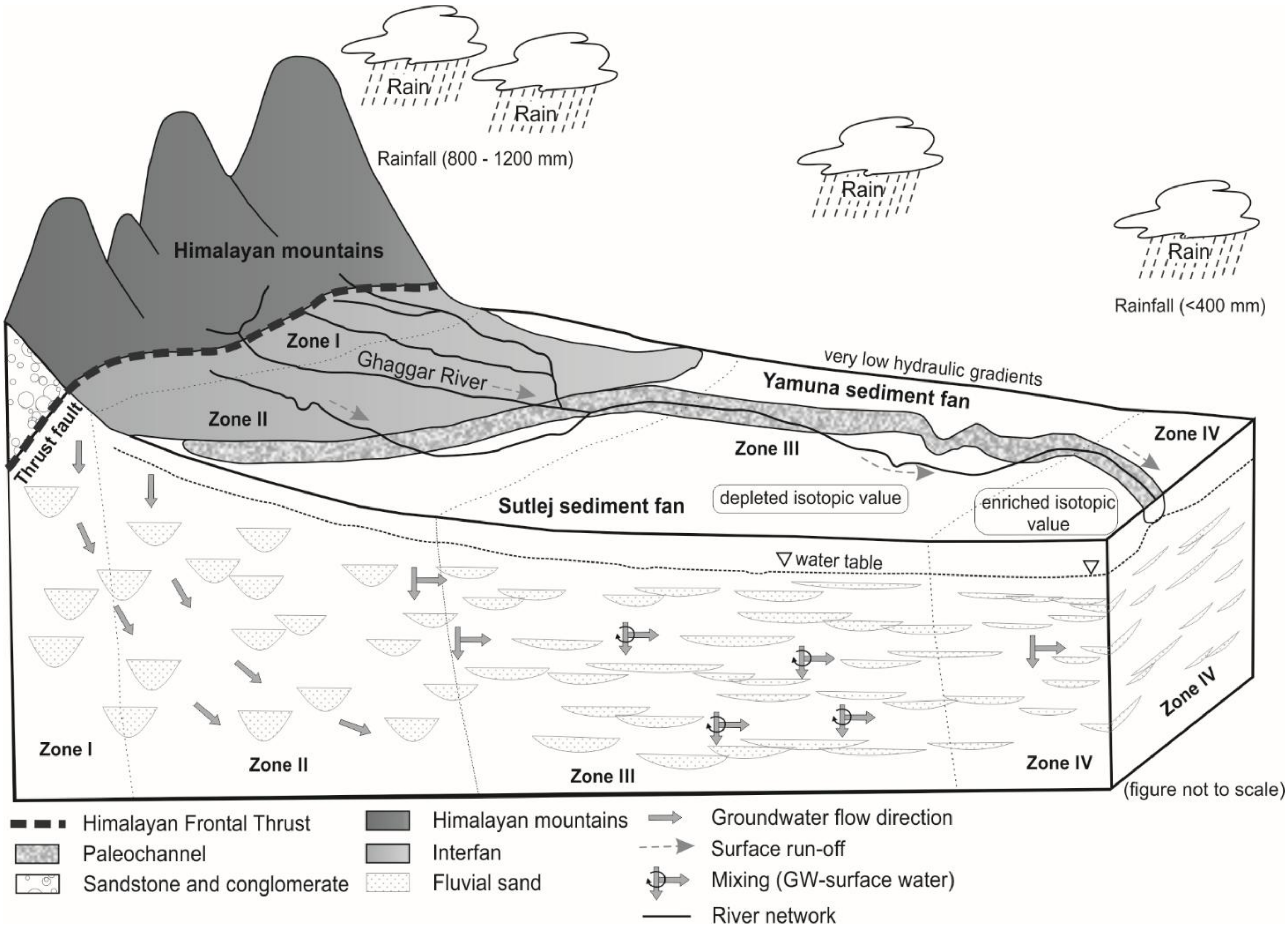
Rain
Rain
Rainfall (800 - 1200 mm)
Rain
Rain
Rainfall (<400 mm)
Himalayan mountains
Zone I
Ghaggar River
Zone II
Thrust fault
very low hydraulic gradients
Yamuna sediment fan
Zone III
Zone IV
Sutlej sediment fan
depleted isotopic value
enriched isotopic value
water table
Zone I
Zone II
Zone III
Zone IV
Zone IV
(figure not to scale)
Himalayan Frontal Thrust
Paleochannel
Sandstone and conglomerate
Himalayan mountains
Interfan
Fluvial sand
Groundwater flow direction
Surface run-off
Mixing (GW-surface water)
River network

Supplementary Figure

Figure S1. The cross plot of δ^{18}O and δ^{2}H of precipitation (grey open squares) for three rain-gauge stations, the local meteoric water line (LMWL) shown by black continuous line, and the global meteoric water line (GMWL) shown by grey continuous line, and the rain-gauge stations are: a) Chandigarh, b) Patiala, and c) Sirsa.

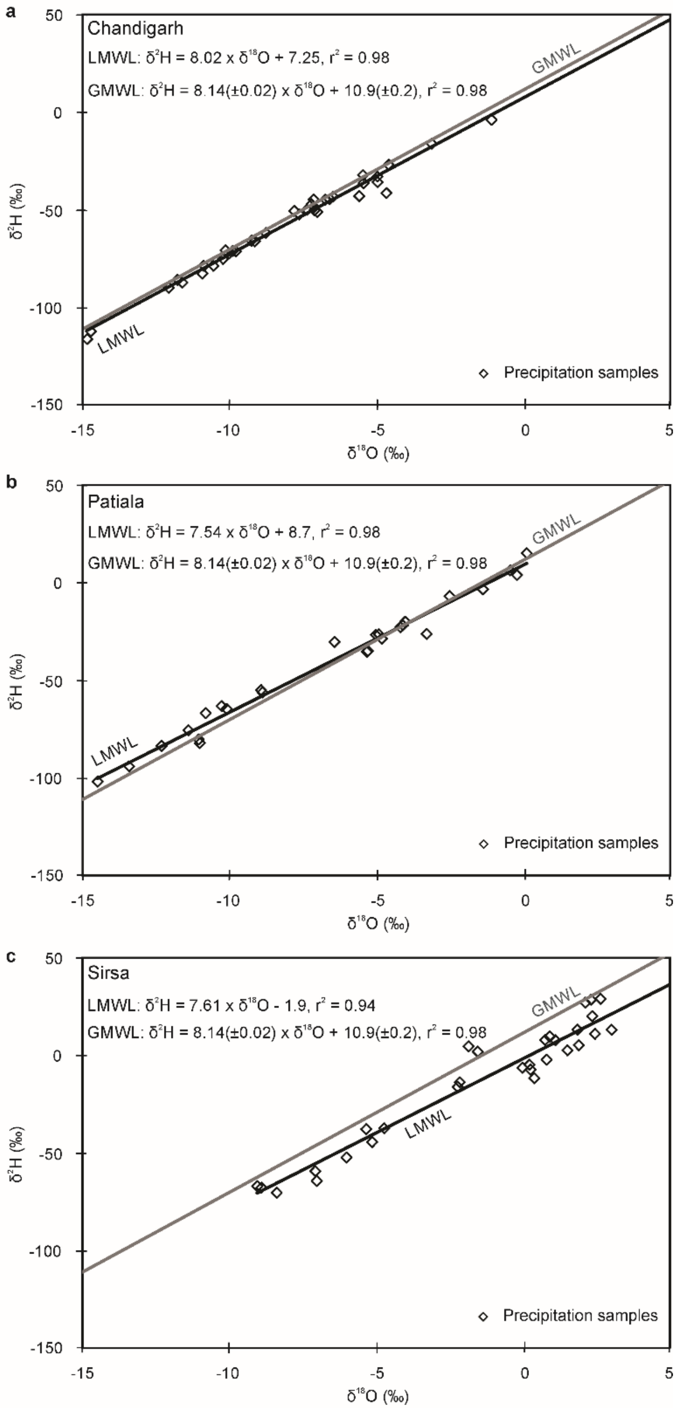

Figure S2. Spatial distribution of water table contours (in meter above sea level), shows groundwater flow direction from northeast to southwest in the study area.